Fe Tris(pyrazolyl)borate Complexes

Amine-Functionalized Spin Crossover Building Blocks

Henrik Flötotto,[a] Tim Secker,[a] Paul Kögerler,*[a] and Claire Besson*[a,b]

Abstract: Bistable spin crossover complexes such as [Fe{HB(pz)$_3$}$_2$] (pzH = pyrazole) show promise for sensor applications and electrically-controlled data storage units, but exploiting their potential hinges on their integration into a functional environment. We here present a system enabling such covalent post-functionalization steps in both symmetric and asymmetric patterns, based on the amine-functionalized complex [Fe{HB-(4-NH$_2$pz)(pz)$_2$}$_2$], obtained by reduction of the nitro analogue. The building block aspects of [Fe{HB(4-NH$_2$pz)(pz)$_2$}$_2$] are show-

cased by its transformation into amide, imine and azo derivatives, which are structurally and magnetically characterized. All tris(pyrazolyl)borate complexes retain the spin crossover properties of their parent compound, with spin crossover temperatures ranging from 350 to 430 K. The transition parameters are correlated with the electronic properties of the functionalizing group, opening the possibility of fine-tuning the spin crossover properties of the building block as it is integrated in the environment of choice.

Introduction

Spin crossover (SCO) complexes, formed by combination of a transition metal cation with an electronic configuration between $3d^4$ and $3d^7$ and ligands of appropriate ligand field strength, can be triggered to transition between two different (meta)stable, low- and high-spin states, e.g. by temperature, pressure or light.[1–3] This translates into potential applicability for room temperature-operable molecular electronics, sensors and displays, which prompted extensive studies on multiple families of SCO complexes.[4–7] Given the pronounced sensitivity of most SCO compounds to minute changes in structure and environment, a key challenge remains: the functionalization of complexes enabling their facile integration via covalent links in a variety of materials relevant to the respective application while retaining their SCO characteristics.[8] While SCO complexes exist for a variety of transition metals and coordination environments, the most commonly observed combination is that of an iron(II) center in an octahedral N$_6$ coordination environment.[9] SCO here results in a large change from a diamagnetic singlet to a paramagnetic $S = 2$ state. We started with the charge-neutral spin crossover complex [Fe{HB(pz)$_3$}$_2$] (**7**, pzH = pyrazole) that undergoes a relatively robust spin transition

around room temperature and proved particularly stable against light, electromagnetic fields, air and water, rendering it a promising target.[10–13]

Poly(pyrazolyl)borate ligands, often termed scorpionates due to their tridentate coordination mode, have found their way into virtually all areas of coordination chemistry since their initial description in 1966 by S. Trofimenko.[14] A considerable number of substituted pyrazolylborate derivatives has been produced, mostly with the objective of modifying the steric and electronic properties of the ligand.[15,16] However, very little work has been dedicated to the introduction of a reactive functionality on that framework.[17] Claims have been made of the synthesis of 5-aminoindazolylborates directly from amino-indazole and tetrahydroborate, alas without structural evidence.[18] We here describe the synthesis of an amine-bearing iron tris(pyrazolyl)borate complex and demonstrate its facile post-functionalization via the formation of amide, imine, diazonium and azo derivatives.
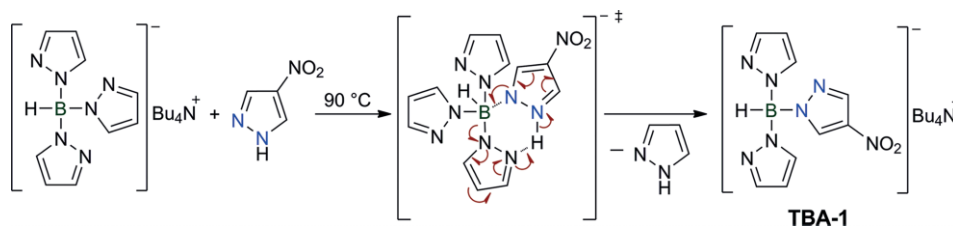
Results and Discussion

The classical poly(pyrazolyl)borate synthesis method, i.e. direct reaction of borohydride with the targeted pyrazole in the melt, was not suitable for our pyrazole candidate, 4-aminopyrazole (4-NH$_2$-pzH), due to the reactivity of the primary amine with the borohydride. We thus targeted 4-nitropyrazole (4-NO$_2$-pzH) as a precursor of the amine function. However, reaction of 4-NO$_2$-pzH with borohydride salts invariably yielded *O*-borate products, as indicated by a single ^{1}H NMR and two ^{13}C NMR signals instead of the patterns (2 signals in ^{1}H, 3 in ^{13}C NMR) expected for less symmetrical *N*-borates. Turning to the much less studied heterocycle metathesis method proved more fruitful. In this case, an N-heterocycle of choice is introduced into a scorpionate structure by substitution of a pyrazole unit from a (preformed) tris(pyrazolyl)borate complex such as [HB(pz)$_3$]$^-$ or [HB(3,5-Me$_2$pz)$_3$]$^-$ (Scheme 1).

[a] H. Flötotto, Dr. T. Secker, Prof. Dr. P. Kögerler, Prof. Dr. C. Besson
Institut für Anorganische Chemie, RWTH Aachen University,
52074 Aachen, Germany
E-mail: paul.koegerler@ac.rwth-aachen.de
[b] Prof. Dr. C. Besson
Department of Chemistry, The George Washington University,
Washington DC 20052 USA
E-mail: Claire_Besson@gwu.edu
Supporting information and ORCID(s) from the author(s) for this article are available on the WWW under https://doi.org/10.1002/ejic.201900916.

ChemPubSoc
Europe

EurJIC
European Journal
of Inorganic Chemistry

Communication
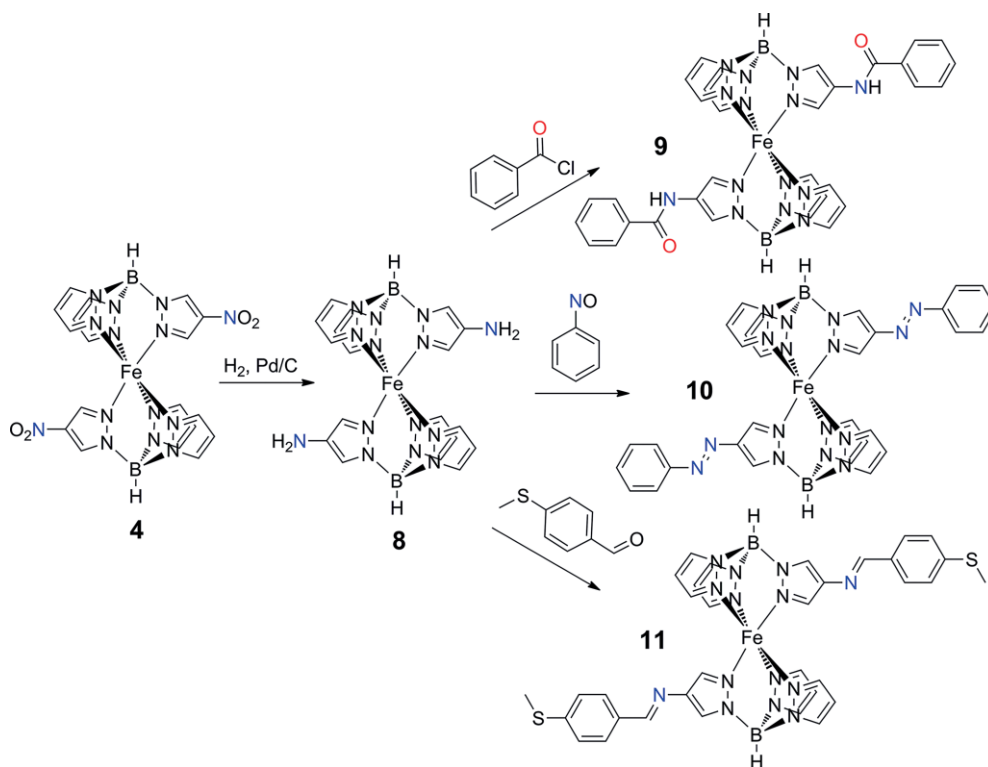
Scheme 1. Ligand functionalization via pyrazole exchange in a HB(pz)$_3^-$ unit.

Despite the relative lability of the B–N bond, this reaction usually requires high temperatures and is poorly selective, yielding mixtures of products with varied substitution patterns.[19–21] However, the reaction of 4-NO$_2$-pzH with K[HB(pz)$_3$] in a non-protic solvent at 60 °C for 2 hours affords K[HB-(4-NO$_2$pz)(pz)$_2$] (K-1) in 70 % yield. Moreover, if the potassium cations of the pyrazolylborate are exchanged for tetra(n-butyl)ammonium (TBA), the reaction can be conducted in solvent-free conditions at 90 °C, and (nBu$_4$N)[HB(4-NO$_2$pz)(pz)$_2$] (TBA-1) is obtained quantitatively. Several parameters contribute to the selectivity of the reaction: We propose that the relative stability of the six-membered ring transition state intermediate proposed in Scheme 1 accounts for the exclusive formation of the N-borate. Selectivity in the formation of the ligand with one nitro function is in line with HSAB theory: due to the charge delocalization permitted by the nitro group, pz$^-$ is a harder base than 4-NO$_2$pz$^-$, while H$^+$, HB(4-NO$_2$pz)(pz) and HB(pz)$_2$ are progressively softer acids. Further substitution can be achieved by varying the stoichiometry and raising the temperature, yielding (nBu$_4$N)[HB(4-NO$_2$pz)$_2$(pz)] (TBA-2) and

(nBu$_4$N)[HB(4-NO$_2$pz)$_3$] (TBA-3; see SI for full experimental details).

[Fe{HB(4-NO$_2$pz)pz$_2$}$_2$] (4, Scheme 2) and [Fe{HB(4-NO$_2$pz)$_2$pz}$_2$] (5) are easily formed by reaction of TBA-1 or TBA-2 with FeCl$_2$ in THF. Asymmetric heteroleptic complexes such as [Fe{HB(4-NO$_2$pz)$_2$pz}(HBpz$_3$)] (6) can be obtained as components of a mixture by reaction of the appropriate ligands and separated from symmetric complexes (e.g. 4 and 7) by column chromatography.

Reduction of the nitro groups of 4 by H$_2$ in the presence of Pd/C produces the targeted diamine complex [Fe{HB(4-NH$_2$pz)(pz)$_2$}$_2$] (8, Scheme 2) in good yield when a protic solvent such as methanol is used. Compound 8 represents an ideal building block as it displays considerable stability towards hydrolysis of the ligand framework and decomplexation of the metal and can thus be engaged in a wide range of reactions characteristic of aromatic amines (Scheme 2). Compound 8 reacts with benzoyl chloride to the amide derivative 9, with nitrosobenzene to the diazene 10, with 4-methylthiobenzaldehyde to the imine 11, and with isopentylnitrite/BF$_3$·THF to the diazonium salt 12.

Scheme 2. Derivatization of nitro derivative 4.

ChemPubSoc
Europe

EurJIC
European Journal
of Inorganic Chemistry

Communication

While complexes **4** – **11** could be characterized structurally and magnetically (see below), we were unsuccessful in growing a single crystal of **12** of sufficient quality for X-ray diffraction. The characterization of this relatively unstable complex was therefore limited to mass spectrometry and IR spectroscopy. Reaction of **12** with iodide and formation of the corresponding iodo derivative was also observed by mass spectrometry. The structures of compounds **4**, **5·2thf**, **6·0.5C$_6$H$_{12}$**, **8**, **9·2Et$_2$O**, **10** and **11** were determined by single-crystal X-ray diffraction (CCDC numbers see below; Figure 1 and SI), bulk purity was confirmed by powder X-ray diffraction (SI). The Fe center is octahedrally coordinated in all species, with a narrow distribution of Fe–N distances [1.954(3) – 1.979(4) Å at 100 K] in the range characteristic for low-spin Fe^{II} species.[22] All complexes except *cis*-dinitro derivative **6** have crystallographically imposed centrosymmetry. While in complexes **4**, **5·2thf**, **9·2Et$_2$O**, **10** and **11** only one half complex defines the asymmetric unit (with the addition of a THF molecule in **5**, and an Et$_2$O molecule hydrogen-bound to the hydrogen of the amide function in **9**), the amine derivative **8** contains two crystallographically distinct half complexes in the asymmetric unit, one of which presents some disorder in the location of the amine group between the three pyrazoles of the ligand.
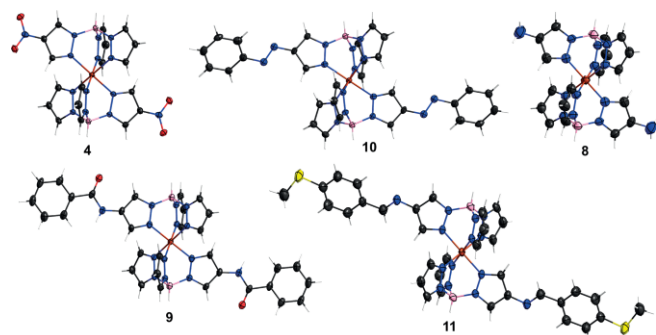

Figure 1. Solid-state structures of complexes **4** and **9**–**11**. Thermal ellipsoids are shown at 50 % probability. Color code: Fe, brown; B, pink; C, black; H, white; N, blue; O, red; S, yellow. Crystal solvent molecules are not shown for clarity.

The magnetic properties of complexes **4** – **6** and **8** – **11** were investigated by SQUID magnetometry between 4 and 480 K (Figure 2 and SI). All compounds display a slow SCO, with no hysteresis, starting above room temperature (Table 1). The supramolecular structure of the compounds, which is usually considered to be the most important contribution to the steepness of the transition, does not appear to have a major impact here (see SI for structural packing effects). On the contrary, despite the 3D network of hydrogen bonds between the amine groups of complex **8**, this derivative shows a markedly lower slope than all other derivatives with the exception of the imine derivative **11**. Amide derivative **9**, with a crystal compacity of 62.9 % and a shortest complex complex interaction of 2.52 Å (O•••H–C) forming a 2D sheet before crystallization solvent loss, presents as steep a transition as the compacter (66.1 %) nitro complex **4**, where a 2D sheet is formed by shortest complex complex interactions of 2.49 Å (O•••H–C) and 2.53 Å (O•••H–C).

No correlation was observed either between the structural parameters of the complexes themselves and the nature of the
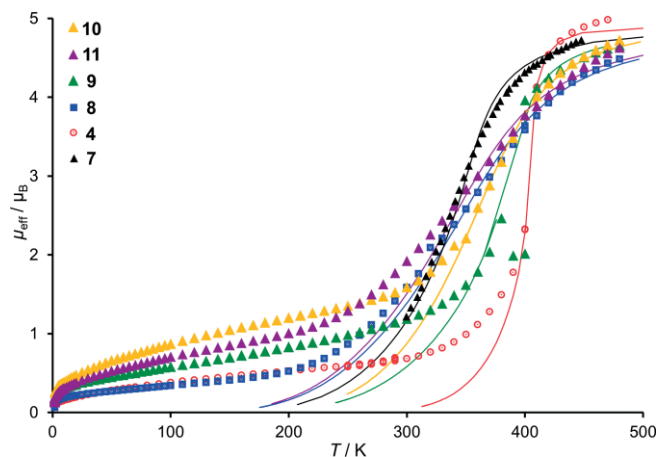

Figure 2. Temperature dependence of the molecular magnetic moment of complexes **4**, **7**,[24] **8**, **9**, **10**, and **11** with fits based on the Schlichter-Drickamer model.

Table 1. SCO parameters.

	4	**7**[24]	**8**	**9**	**10**	**11**
$T_{1/2}$ / K	401	339	345	376	357	338
$\Delta_r H$ / kJ mol^{-1}	69.0	23.4	19.4	26.0	31.0	19.0
$\Delta_r S$ / J mol^{-1} K^{-1}	170	65	50	66	80	50
Γ / kJ mol^{-1}	5.8	3.5	2.0	4.5	1.6	2.0

SCO. We then turned our attention to the electronic effect of the group functionalizing the tris(pyrazolyl)borate framework. In order to decouple the position and steepness of the transition, the magnetic data was fitted to a regular solution model by Schlicher and Drickamer,[23] extracting enthalpy and entropy for the spin transition (Table 1, $\Delta_r H$ and $\Delta_r S$) as well as mixing enthalpy between the high-spin and low-spin complexes (Table 1, Γ). Note that those values are purely empirical and are not expected to be a realistic representation of the actual thermodynamic SCO parameters, only to correlate with them. A reasonable correlation was found between the donor ability of the substituent of *trans* disubstituted derivatives **4** and **7** – **11**, modeled by the pK_a of the corresponding pyrazole, and the singlet-quintet enthalpy difference $\Delta_r H$ (Figure 3). The sign
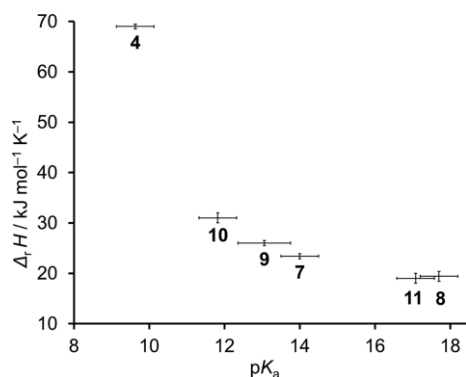

Figure 3. Hammett-type plot of the dependence of the fitted enthalpy difference between low and high spin as a function of the calculated pK_a[25] of the corresponded substituted pyrazole.

of the correlation, however, is surprising. As tris(pyrazolyl)borates are essentially σ-donating ligands, we would expect that a donor substituent on the pyrazole, increasing its pK_a and its σ-donating strength, would increase the single-quintet energy gap of the iron complex. The opposite is observed, and the highest singlet-quintet enthalpy difference, and SCO temperature, is observed for the nitro-substituted complex.

Trans and *cis* disubstituted nitro derivatives **4** and **6** show very similar transitions (cf. SI), also in agreement with a primarily electronic effect of the substituents. Finally, the tetra-substituted nitro complex **5** displays the highest $T_{1/2}$ of all complexes, but the relatively poor quality of the fit precludes further analysis of its properties.

Conclusions

In summary, the amine-substituted Fe^{II} tris(pyrazolyl)borate complex **8** was isolated and demonstrated to retain the SCO properties of its parent non-functionalized compound upon post-functionalization into amide, imine, and azo derivatives without losing its spin transition, rendering it an ideal building block for the covalent integration of spin crossover properties in a variety of materials, including polymers and hybrid materials. The wide range of functionalities accessible from an amine group, coupled with an extension of the pyrazole metathesis method perfected here to include different pyrazole substrates and both symmetric and asymmetric substitution patterns in the resulting Fe^{II} complexes, should enable in-depth studies of the tuning of SCO properties by the electronic effect of the substituent, a departure from the traditional approach relying on steric and crystal packing effects. Finally, the approach developed here for iron complexes could be extended to other transition metals as well as lanthanoid cations, widening the range of range of properties available to single-molecule magnetism and catalysis.

CCDC 1822138 (for **4**), 1859383 (for **5·2thf**), 1859382 (for **6·0.5C$_6$H$_{12}$**), 1822139 (for **8**), 1822140 (for **9·2Et$_2$O**), 1822141 (for **10**), and 1822142 (for **11**) contain the supplementary crystallographic data for this paper. These data can be obtained free of charge from The Cambridge Crystallographic Data Centre.

[1] *Spin Crossover in Transition Metal Compounds I-III*, *Topics in Current Chemistry Vol. 233–235* (Eds.: P. Gütlich, H. A. Goodwin), Springer Verlag, Berlin-Heidelberg, **2004**.

[2] *Spin-Crossover Materials: Properties and Applications* (Ed.: M. A. Halcrow), John Wiley & Sons, Chichester, **2013**.

[3] K. Senthil Kumar, I. Šalitroš, B. Heinrich, O. Fuhr, M. Ruben, *J. Mater. Chem. C* **2015**, *3*, 11635–11644.

[4] K. S. Kumar, M. Studniarek, B. Heinrich, J. Arabski, G. Schmerber, M. Bowen, S. Boukari, E. Beaurepaire, J. Dreiser, M. Ruben, *Adv. Mater.* **2018**, *30*, 1705416.

[5] E. Coronado, J. R. Galán-Mascarós, M. Monrabal-Capilla, J. García-Martínez, P. Pardo-Ibáñez, *Adv. Mater.* **2007**, *19*, 1359–1361.

[6] C. Lefter, S. Rat, J. S. Costa, M. D. Manrique-Juárez, C. M. Quintero, L. Salmon, I. Séguy, T. Leichle, L. Nicu, P. Demont, A. Rotaru, G. Molnár, A. Bousseksou, *Adv. Mater.* **2016**, *28*, 7508–7514.

[7] P. Gamez, J. S. Costa, M. Quesada, G. Aromí, *Dalton Trans.* **2009**, 7845–7853.

[8] K. Senthil Kumar, M. Ruben, *Coord. Chem. Rev.* **2017**, *346*, 176–205.

[9] P. Gütlich, A. B. Gaspar, Y. Garcia, *Beilstein J. Org. Chem.* **2013**, *9*, 342–391.

[10] J. P. Jesson, S. Trofimenko, D. R. Eaton, *J. Am. Chem. Soc.* **1967**, *89*, 3158–3164.

[11] F. Grandjean, G. J. Long, B. B. Hutchinson, L. Ohlhausen, P. Neill, J. D. Holcomb, *Inorg. Chem.* **1989**, *28*, 4406–4414.

[12] T. Mahfoud, G. Molnár, S. Cobo, L. Salmon, C. Thibault, C. Vieu, P. Demont, A. Bousseksou, *Appl. Phys. Lett.* **2011**, *99*, 053307.

[13] T. Zhao, I. Boldog, V. Spasojevic, A. Rotaru, Y. Garcia, C. Janiak, *J. Mater. Chem. C* **2016**, *4*, 6588–6601.

[14] S. Trofimenko, *J. Am. Chem. Soc.* **1966**, *88*, 1842–1844.

[15] *Scorpionates: The Coordination Chemistry of Polypyrazolylborate Ligands* (Ed.: S. Trofimenko), Imperial College Press, London, **1999**.

[16] *Scorpionates II: chelating borate ligands* (Ed.: C. Pettinari), Imperial College Press, London, **2008**.

[17] D. L. Reger, J. R. Gardinier, W. R. Gemmill, M. D. Smith, A. M. Shahin, G. J. Long, L. Rebbouh, F. Grandjean, *J. Am. Chem. Soc.* **2005**, *127*, 2303–2316.

[18] K. S. Siddiqi, M. A. Neyazi, S. T. Lutfullah, S. A. A. Zaidi, *Indian J. Chem.* **1991**, *30A*, 724–726.

[19] T. Ruman, M. Łukasiewicz, Z. Ciunik, S. Wołowiec, *Polyhedron* **2001**, *20*, 2551–2558.

[20] B. Benkmil, M. Ji, H. Vahrenkamp, *Inorg. Chem.* **2004**, *43*, 8212–8214.

[21] P. J. Desrochers, B. M. Besel, A. L. Corken, J. R. Evanov, A. L. Hamilton, D. L. Nutt, R. M. Tarkka, *Inorg. Chem.* **2011**, *50*, 1931–1941.

[22] P. Gütlich, A. Hauser, H. Spiering, *Angew. Chem. Int. Ed. Engl.* **1994**, *33*, 2024–2054; *Angew. Chem.* **1994**, *106*, 2109–2141.

[23] C. P. Slichter, H. G. Drickamer, *J. Chem. Phys.* **1972**, *56*, 2142–2160.

[24] L. Salmon, G. Molnár, S. Cobo, P. Oulié, M. Etienne, T. Mahfoud, P. Demont, A. Eguchi, H. Watanabe, K. Tanaka, A. Bousseksou, *New J. Chem.* **2009**, *33*, 1283–1289.

[25] pK_a values calculated using Advanced Chemistry Development (ACD/Labs) Software v11.02.